

© [2007] IEEE. Reprinted, with permission, from [Yong Zhang, Shao, K.R.; Youguang Guo; Jianguo Zhu; Xie, D.X.; Lavers, J.D., A Comparison of Point Interpolative Boundary Meshless Method Based on PBF and RBF for Transient Eddy-Current Analysis, Magnetics, IEEE Transactions on (Volume:43 , Issue: 4 ), April 2007]. This material is posted here with permission of the IEEE. Such permission of the IEEE does not in any way imply IEEE endorsement of any of the University of Technology, Sydney's products or services. Internal or personal use of this material is permitted. However, permission to reprint/republish this material for advertising or promotional purposes or for creating new collective works for resale or redistribution must be obtained from the IEEE by writing to [pubs-permissions@ieee.org](mailto:pubs-permissions@ieee.org). By choosing to view this document, you agree to all provisions of the copyright laws protecting it

# **A Comparison of Point Interpolative Boundary Meshless Method Based on PBF and RBF for Transient Eddy Current Analysis**

*Yong Zhang, K.R. Shao*

Huazhong Univ. of Sci. & Tech., Wuhan, 430074, P.R. China

*Youguang Guo*

University of Technology, Sydney, NSW 2007, Australia

*D.X. Xie*

Shenyang University of Technology, Shenyang 110023 P.R.China

*J.D. Lavers*

University of Toronto, Toronto, Ont. M5S 3G4, Canada

***Abstract*** -- This paper presents boundary polynomial point interpolation meshless method (BPPIM) and boundary radial point interpolation meshless method (BRPIM) based on polynomial basis function (PBF) and radial basis function (RBF) respectively for transient eddy current analysis, and their interpolation shape functions satisfy the Kronecker delta function, thus the essential boundary conditions can be directly imposed on the boundary nodes. An example on analyzing transient eddy current of a square metal column is set to prove the validity of the proposed methods, and a comparison on accuracy between BPPIM and BRPIM is analyzed as well.

## I. INTRODUCTION

**Boundary meshless methods (BMMs) are attractive and important computational techniques for reducing the dimensionality of the solving problems. Several boundary-type meshless methods have been developed for many potential and elastic problems [1] ~ [2], they need no discretization of the boundary and are proven as robust numerical methods. But very few of them are used to solve electromagnetic problems, say nothing of transient eddy current problems. A work of BMMs for transient eddy current problems has been recently published by the authors [3]. In this paper, boundary polynomial point interpolation meshless method (BPPIM) and boundary radial point interpolation meshless method (BRPIM) based on polynomial basis function (PBF) and radial basis function (RBF) are presented respectively for transient eddy current analysis, and both their interpolation shape functions satisfy the Kronecker delta function, thus the essential boundary conditions can be**

directly imposed on the boundary nodes. For comparing BPPIM and BRPIM, an example on analyzing transient eddy current of a square metal column is illustrated, and accuracy analysis between them are expounded as well.

## II. Point Interpolation on Curves

### A. Polynomial basis point interpolation method (PPIM)

Consider a two-dimensional domain  $\Omega$  with boundary  $\Gamma$ , as shown in Fig.1. In using boundary meshless method, only the boundary  $\Gamma$  of the problem domain is represented using nodes. The point interpolation method (PIM) is constructed on the one-dimensional bounding curve  $\Gamma$  of two-dimensional domain  $\Omega$ , using a set of discrete nodes on  $\Gamma$ . As in the conventional BEM method,

**u** and **q** are constructed independently using PIM shape function as

$$u(s) = \sum_{j=1}^m p_j(s) a_j = \mathbf{p}^T(s) \cdot \mathbf{a} \quad , \quad q(s) = \sum_{j=1}^m p_j(s) b_j = \mathbf{p}^T(s) \cdot \mathbf{b} \quad (1)$$

**In matrix form, there are**

$$\mathbf{a} = [a_1, a_2, \dots, a_m]^T \quad \mathbf{b} = [b_1, b_2, \dots, b_m]^T \quad \mathbf{p}(s) = [1, s, \dots, s^{m-1}]^T \quad (2)$$

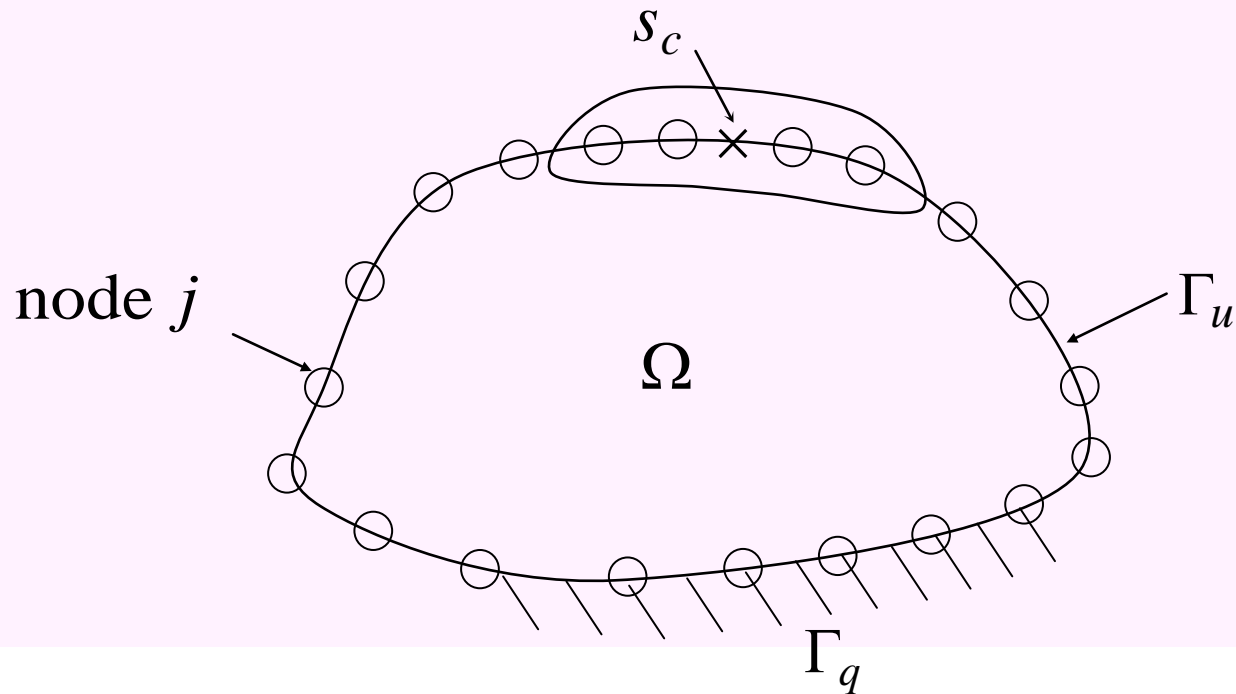


**Fig.1 Problem domain and boundary and nodes**

The coefficient  $a_j$  and  $b_j$  in (2.a) and (2.b) can be determined by enforcing (1.a) and (1.b) to be satisfied at the  $m$  nodes surrounding the point  $s_c$ . Equation (1) can then be written in the following matrix form

$$\mathbf{u}_m = \mathbf{P}_c \mathbf{a} \quad (3.a)$$

$$\mathbf{q}_m = \mathbf{P}_c \mathbf{b} \quad (3.b)$$

In (3.a) and (3.b), we have

$$\mathbf{u}_m = [u_1, u_2, \dots, u_m]^T \quad (4.a)$$

$$\mathbf{q}_m = [q_1, q_2, \dots, q_m]^T \quad (4.b)$$

$$\mathbf{P}_c = [\mathbf{p}(s_1), \mathbf{p}(s_2), \dots, \mathbf{p}(s_m)]^T \quad (4.c)$$

Solving **a** and **b** from (3.a) and (3.b), then we can obtain

$$u(s) = \Phi^T(s) \mathbf{u}_m \quad (5.a)$$

$$q(s) = \Phi^T(s) \mathbf{q}_m \quad (5.b)$$

### *B. Radial basis point interpolation method (RPIM)*

To radial basis function point interpolation method, (1) can be rewritten as

$$u(s) = \sum_{i=1}^n R_i(s) a_i + \sum_{j=1}^m p_j(s) b_j = \mathbf{R}^T(s) \mathbf{a} + \mathbf{p}^T(s) \mathbf{b} \quad (6.a)$$

$$q(s) = \sum_{i=1}^n R_i(s) c_i + \sum_{j=1}^m p_j(s) d_j = \mathbf{R}^T(s) \mathbf{c} + \mathbf{p}^T(s) \mathbf{d} \quad (6.b)$$

Where  $R_i(s) = (s_i^2 + c)^q$  in this paper, the parameters and basis

in matrix form are

$$\mathbf{a} = [a_1, a_2, \dots, a_n]^T \quad \mathbf{b} = [b_1, b_2, \dots, b_m]^T \quad \mathbf{c} = [c_1, c_2, \dots, c_n]^T \quad (7.a)$$

$$\mathbf{R}(s) = [R_1(s), R_2(s), \dots, R_n(s)]^T \quad (7.b)$$

$$\mathbf{d} = [d_1, d_2, \dots, d_m]^T \quad \mathbf{p}(s) = [1, s, \dots, s^{m-1}]^T \quad (7.c)$$

For the uniqueness of the radial point interpolation, the relationship should be satisfied as following

$$\sum_{i=1}^n p_j(s) a_i = \mathbf{P}_0^T \mathbf{a} = 0 \quad \sum_{i=1}^n p_j(s) c_i = \mathbf{P}_0^T \mathbf{c} = 0 \quad (j = 1, 2, \dots, m) \quad (8)$$

Combining (6) (8) get the matrix form of the parameters are

$$\begin{bmatrix} \mathbf{R}_0 & \mathbf{P}_0 \\ \mathbf{P}_0^T & 0 \end{bmatrix} \begin{bmatrix} \mathbf{a} \\ \mathbf{b} \end{bmatrix} = \mathbf{G} \begin{bmatrix} \mathbf{a} \\ \mathbf{b} \end{bmatrix} = \begin{bmatrix} \mathbf{u}_n \\ 0 \end{bmatrix} \quad \begin{bmatrix} \mathbf{R}_0 & \mathbf{P}_0 \\ \mathbf{P}_0^T & 0 \end{bmatrix} \begin{bmatrix} \mathbf{c} \\ \mathbf{d} \end{bmatrix} = \mathbf{G} \begin{bmatrix} \mathbf{c} \\ \mathbf{d} \end{bmatrix} = \begin{bmatrix} \mathbf{q}_n \\ 0 \end{bmatrix} \quad (9)$$

And the unknown parameters are solved from (9) as

$$\begin{bmatrix} \mathbf{a} \\ \mathbf{b} \end{bmatrix} = \mathbf{G}^{-1} \begin{bmatrix} \mathbf{u}_n \\ 0 \end{bmatrix} \quad \begin{bmatrix} \mathbf{c} \\ \mathbf{d} \end{bmatrix} = \mathbf{G}^{-1} \begin{bmatrix} \mathbf{q}_n \\ 0 \end{bmatrix} \quad (10)$$

Substituting (10) into (6) and get

$$u(s) = [\mathbf{R}^T(s) \mathbf{p}^T(s)] \mathbf{G}^{-1} [\mathbf{u}_n \ 0]^T = \mathbf{\Phi}^T(s) \mathbf{u}_n \quad (11.a)$$

$$q(s) = [\mathbf{R}^T(s) \mathbf{p}^T(s)] \mathbf{G}^{-1} [\mathbf{q}_n \ 0]^T = \mathbf{\Phi}^T(s) \mathbf{q}_n \quad (11.a)$$

The matrix form of shape function  $\mathbf{\Phi}(s)$  both in PPIM and in RPIM are defined by

$$\mathbf{\Phi}^T(s) = [\phi_1(s), \phi_2(s), \dots, \phi_n(s)] \quad (12)$$

And equation (5) and (11) can be written as

$$u(s) = \sum_{i=1}^n \phi_i(s) u_i, \quad q(s) = \sum_{i=1}^n \phi_i(s) q_i \quad (13)$$

The shape functions are formed by RPIM should be more

complicated than those by PPIM, but the latter one may gain less accuracy than the former one, in which some parameters are required to be determined carefully because they directly affect the accuracy and the performance of the RPIM.

The shape functions  $\phi(s)$  both in (5) and (11) satisfy Kronecker delta function as

$$\phi_j(s_i) = \delta_{ji} = \begin{cases} 1 & i = j \\ 0 & i \neq j \end{cases}, \quad \sum_{j=1}^m \phi_j(s) = 1 \quad (14)$$

Therefore, the shape functions constructed have the Kronecker delta function property, and the essential boundary conditions can be easily imposed as in traditional BEM.

### III. Transient Eddy Current Problem

The full set of equations for low-frequency electromagnetic field can be now written as

$$\nabla \times \mathbf{E} = -\frac{\partial \mathbf{B}}{\partial t}, \quad \nabla \times \mathbf{H} = \mathbf{J}_e + \mathbf{J}_s, \quad \mathbf{B} = \mu \mathbf{H}, \quad \mathbf{J}_e = \sigma \mathbf{E} \quad (15.a)$$

where  $\mathbf{J}_e$  and  $\mathbf{J}_s$  are eddy current and source current respectively. The initial and boundary problems for two-dimensional transient eddy current field is written as

$$\left\{ \begin{array}{ll} \nabla^2 u = \sigma \mu \frac{\partial u}{\partial t} - P & \text{in } \Omega \text{ at } 0 < t < t_n \\ u = \bar{u} & \text{on } \Gamma_u \text{ at } 0 < t < t_n \\ q = \bar{q} & \text{on } \Gamma_q \text{ at } 0 < t < t_n \\ u = u_0 & \text{in } \Omega \text{ at } t = 0 \end{array} \right. \quad (16)$$

## IV.BPPIM and BRPIM Formulations

### A. Discrete equations by BPPIM and BRPIM

The well-known boundary integration equation for two-dimensional linear medium problems is given by

$$c_i(u_i)_{t_n} + \frac{1}{\sigma\mu} \int_0^{t_n} \int_{\Gamma} q^* u \, d\Gamma dt = \frac{1}{\sigma\mu} \int_0^{t_n} \int_{\Gamma} u^* q \, d\Gamma dt + \frac{1}{\sigma\mu} \int_0^{t_n} \int_{\Omega} u^* P \, d\Omega dt + [\int_{\Omega} u^* u \, d\Omega]_{t=0} \quad (17)$$

$$u^* = \frac{\sigma\mu}{4\pi(t_n - t)} \exp\left(-\frac{\sigma\mu r^2}{4\pi(t_n - t)}\right) \quad (18.a)$$

$$q^* = -\frac{(\sigma\mu)^2}{8\pi(t_n - t)^2} \exp\left(-\frac{\sigma\mu r^2}{4\pi(t_n - t)}\right) \frac{\partial r}{\partial n} \quad (18.b)$$

To get the numerical solution of equation (17), time should be discrete into  $N$  time steps for computation

$$u(t) = \sum_{k=1}^l M^k u^k = \mathbf{M}^T \mathbf{u}^t, \quad q(t) = \sum_{k=1}^l M^k q^k = \mathbf{M}^T \mathbf{q}^t \quad (19.a)$$

Where  $u^k$  and  $q^k$  are the values of  $u$  and  $q$  at time  $t = t_k$ ,  $\mathbf{M}^T = [M^1, M^2, \dots, M^l]$  are the shape functions of  $u^k$  and  $q^k$ ,  $\mathbf{u}^t = [u^1, u^2, \dots, u^2]$  and  $\mathbf{q}^t = [q^1, q^2, \dots, q^2]$ .

Substituting (13) and (19) into (17) yields the boundary meshless method for all nodes on the boundary of the problem domain

$$\mathbf{H}^k \mathbf{U}^k = \mathbf{G}^k \mathbf{Q}^k + \mathbf{F}^k \mathbf{P}^k + \mathbf{B} \bar{\mathbf{U}}^0 \quad (24)$$

Where

$$\mathbf{H}^k = \mathbf{c}_i + \frac{1}{\sigma \mu} \int_{t_{k-1}}^{t_k} \int_{\Gamma} \mathbf{q}^* \Phi^T(s) \mathbf{M}^T d\Gamma dt \quad (25.a)$$

$$\mathbf{G}^k = \frac{1}{\sigma \mu} \int_{t_{k-1}}^{t_k} \int_{\Gamma} \mathbf{u}^* \Phi^T(s) \mathbf{M}^T d\Gamma dt \quad (25.b)$$

$$\mathbf{F}^k = \frac{1}{\sigma \mu} \int_{t_{k-1}}^{t_k} \int_{\Omega} \mathbf{u}^* \Phi^T(s) \mathbf{M}^T d\Omega dt, \quad \mathbf{B} = [\int_{\Omega} \mathbf{u}^* d\Omega]_{t=0} \quad (25.c)$$

$$\mathbf{U}^k = [u_1, u_2, \dots, u_n]_{t=t_k}^T, \quad \mathbf{Q}^k = [q_1, q_2, \dots, q_n]_{t=t_k}^T \quad (25.d)$$

$$\mathbf{P}^k = [p_1, p_2, \dots, p_m]_{t=t_k}^T, \quad \bar{\mathbf{U}}^0 = [\bar{u}_1, \bar{u}_2, \dots, \bar{u}_m]_{t=0}^T \quad (25.e)$$

### *B. Operation on singular integral of BPPIM and BRPIM*

The log Gaussian quadrature are required to evaluate the  $\ln(1/x)$  type singular integrals, which are existed in matrix  $\mathbf{G}$ , as follows

$$I = \int_0^1 \ln(1/x) f(x) dx \cong \sum_{k=1}^m f(x_k) w_k \quad (25)$$

Moreover, the  $1/x$  type singular integrals are existed in matrix **H**, it is not a trivial task to get the diagonal terms of matrix **H**. Note that shape functions both of BPPIM and BRPIM possess Kronecker delta function property, therefore, the Rigid Body Movement method can be used here to obtain the diagonal terms of matrix **H**, and the singular integrals in matrix **H** are avoided.

### *C. Nodes distribution and some practical experiences*

Some practical experiences are obtained as follows:

- The nodes near to the load points should be distributed compactly and those far away loosely.
- If boundary conditions with high gradient are imposed, then more compact nodes should be distributed on the load boundaries to precisely

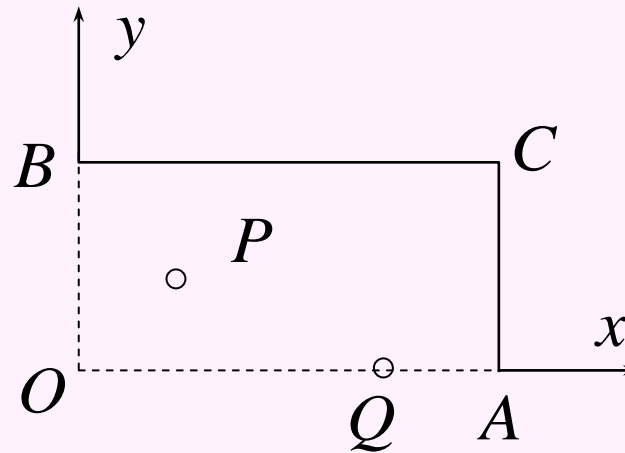
represent the boundary conditions.

- The nodes distributed on the essential boundary and those on the natural boundary should express different boundary characteristics, namely, the nodes for point interpolation on the essential boundaries had better not include those on the natural boundaries, and this rule is also suitable to nodes on the natural boundaries for point interpolation.

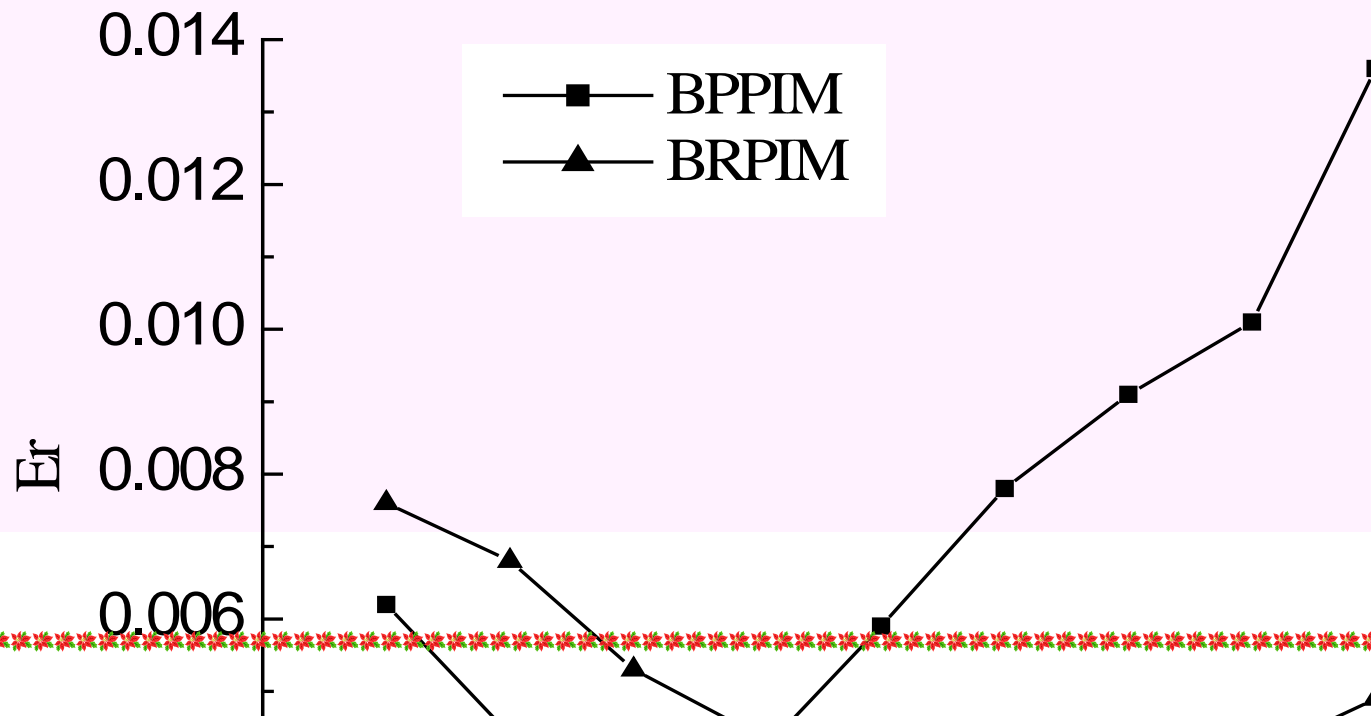
## V. Comparison between BPPIM and BRPIM

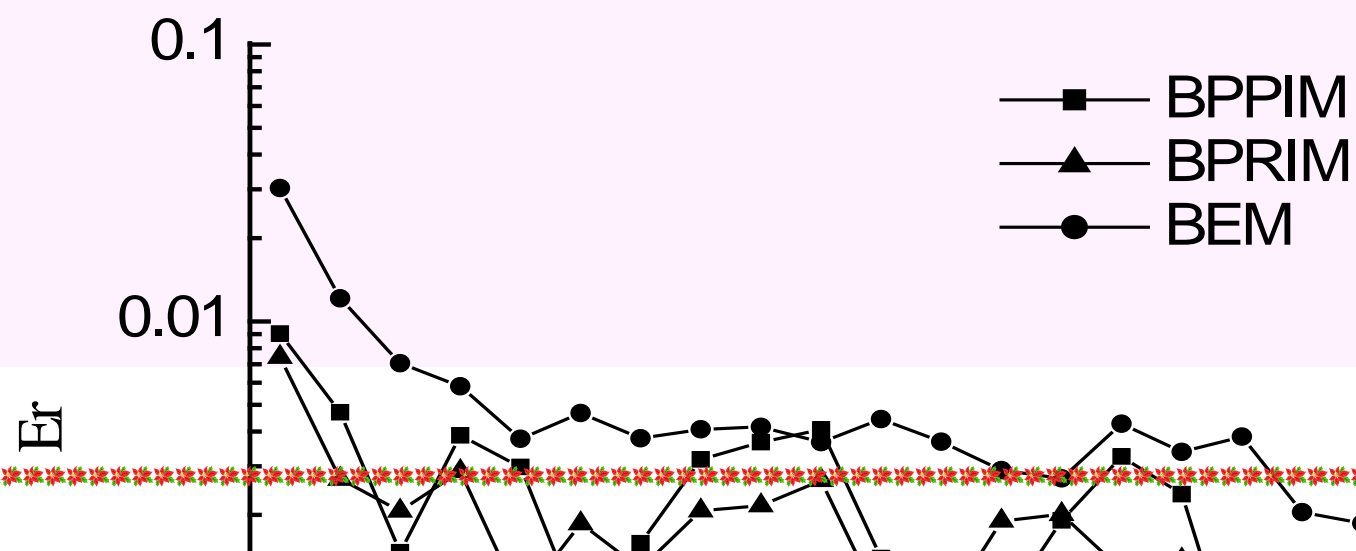
In order to verify the proposed method, a metal column with infinite length is magnetizing here, its cross section of one quadrant is shown as Fig.2. The parameters of the size and the medium type are:  $OA = 0.4$  m,  $OB = 0.2$  m,  $\mu_r = 1000$ ,  $\sigma = 1.04 \times 10^6$  S/m. At time  $t = 0$ , a step magnetic field  $H_0$  with direct  $-z$  is imposed on the outer surface of the metal column. Points P(0.1,0.1) and Q(0.3,0)

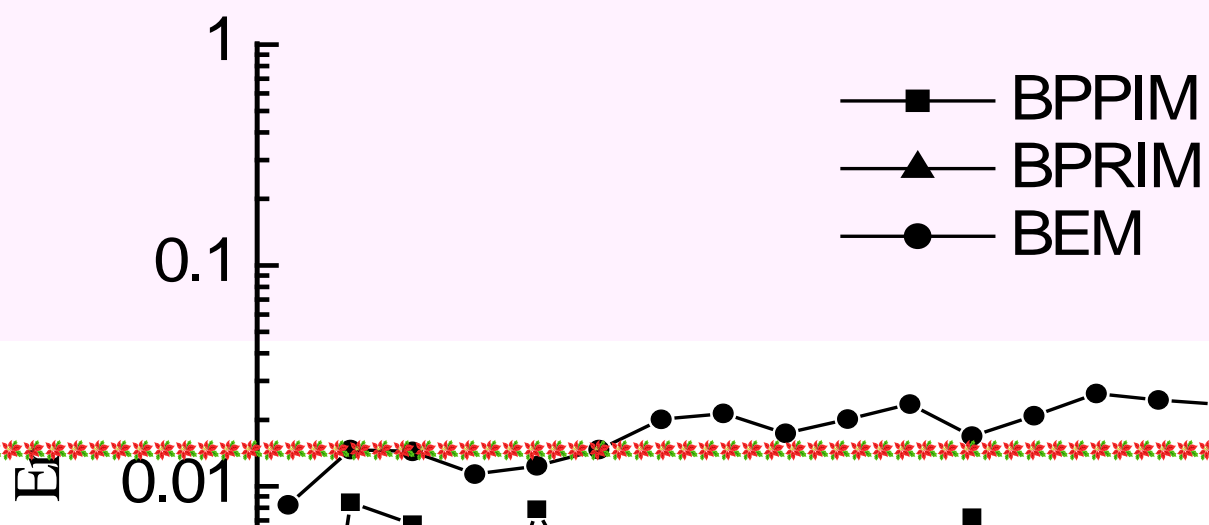
are investigated to compare BPPIM and BRPIM.



**Fig.2 Cross section of one quadrant of the metal column**







## VI. CONCLUSIONS

**Both BPPIM and BRPIM belong to point interpolative boundary meshless method, they are both effective and suitable for**

transient eddy current analysis, and they both have the Kronecker delta function property, and the essential boundary conditions can be easily imposed as in traditional BEM. Based on numerical experiments from this paper, the main difference between these two methods is as follows:

(1) To BPPIM, the number of nodes in support domain for interpolation is  $N_p$ , and the order number of the shape functions is  $N_p-1$ , thus the number  $N_p$  determines the accuracy of results. To BRPIM, it has no such relationship. A suitable number of nodes in support domain for BPPIM is  $N_p=3\sim5$ , but it is  $N_r=5\sim9$  for BRPIM.

(2) The shape functions at each quadrature point include a matrix inversion. Under equal performance of accuracy, there generally has the relationship  $N_p < N_r$ . This also reflects that BPPIM needs less computing time than that of BRPIM.

**(3) The accuracy of BRPIM depends on the parameters of RBF in great degree [4], but to its contrary, BPPIM employs PBF and it independent from any parameter.**

**(4) It is based on the suitable RBF parameters and the relative more computing time that make BRPIM gets more accuracy than that of BPPIM.**